The Abdus Salam
International Centre for Theoretical Physics

United Nations
Educational, Scientific and
Cultural Organization

IAEA
International Atomic Energy Agency

2137-11

Joint ICTP-IAEA Advanced Workshop on Multi-Scale Modelling for Characterization and Basic Understanding of Radiation Damage Mechanisms in Materials

12 - 23 April 2010

Exchange and correlation in Density Functional Theory

J.J. Kohanoff
The Queen's University of Belfast
United Kingdom

EXCHANGE AND CORRELATION IN DENSITY FUNCTIONAL THEORY

JORGE KOHANOFF

LECTURE 2

TOTAL ENERGY

$$E[\rho] = T_R[\rho] + E_H[\rho] + V_{ext}[\rho] + E_{xc}[\rho]$$

$E_{xc}[\rho]$: UNKNOWN

EXCHANGE-CORRELATION ENERGY

$$E_{xc}[\rho] = \frac{1}{2}\iint \frac{\rho(\underline{r})\,\rho(\underline{r}')}{|\underline{r}-\underline{r}'|}\left[\tilde{g}(\underline{r},\underline{r}') - 1\right] d\underline{r}\,d\underline{r}'$$

$\tilde{g}(\underline{r},\underline{r}')$: NON-LOCAL UNKNOWN OBJECT.

LOCAL DENSITY APPROXIMATION (LDA)

$$E_{xc}[\rho] = \int \rho(\underline{r})\,\boxed{\epsilon_{xc}^{LDA}[\rho](\underline{r})}\,d\underline{r}$$

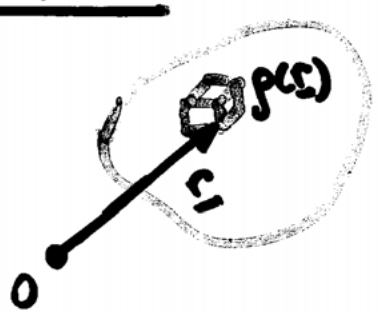

$\epsilon_{xc}^{LDA}[\rho](\underline{r})$: XC ENERGY DENSITY OF HOMOG. ELECTRON GAS

$$\epsilon_{xc}^{LDA}[\rho] = \frac{1}{2}\int \frac{\tilde{\rho}_{xc}^{LDA}(\underline{r},\underline{r}')}{|\underline{r}-\underline{r}'|}\,dr'$$

$$\tilde{g}_{xc}^{LDA}(\underline{r},\underline{r}') = \tilde{g}_{xc}^{h}(|r-r'|, \rho(r))$$

- LDA XC HOLE CENTERED AT $\underline{r}$, INTERACTS WITH ELECTRON AT $\underline{r}$. EXACT XC HOLE CENTERED AT $\underline{r}'$, NOT $\underline{r}$.
- THIS is COMPENSATED BY MULTIPLYING $\tilde{g}_{xc}^{h}$ WITH THE DENSITY RATIO $\rho(r)/\rho(r')$.

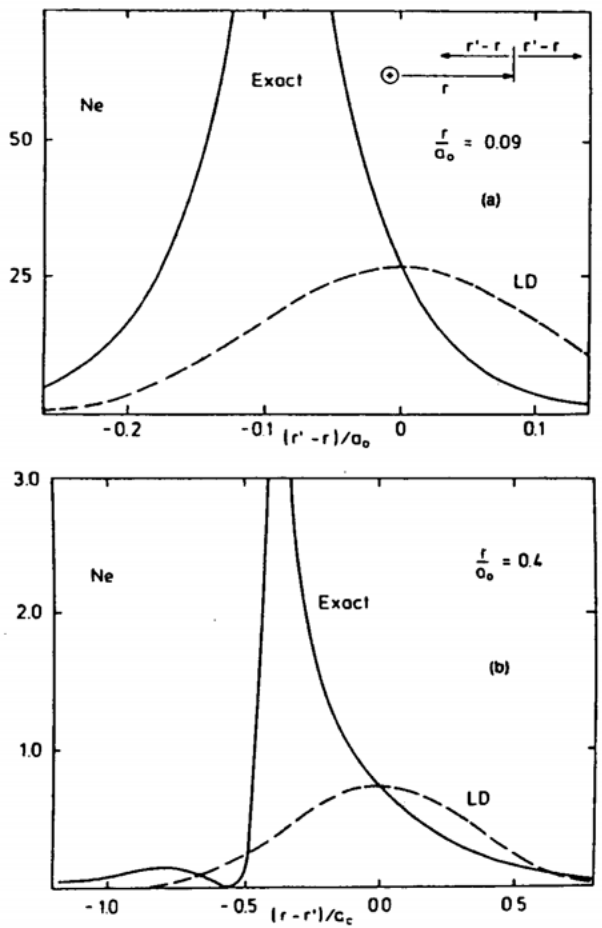

Figure 8.1 Exchange hole $\rho_x(\mathbf{r}, \mathbf{r}')$ for a neon atom. The full curves shown exact results and broken curves show the results in the LD approximation. The curves in (a) and (b) are for two different values of r. (From Gunnarsson, Jonson, and Lundqvist 1979.)

density (WD) method; namely,

$$\rho_{xc}^{\mathrm{WD}}(\mathbf{r}_1, \mathbf{r}_2) = \rho(\mathbf{r}_2)\bar{h}_0(|\mathbf{r}_1 - \mathbf{r}_2|; \bar{\rho}(\mathbf{r}_1)) \tag{8.5.33}$$

where $\bar{\rho}(\mathbf{r}_1)$ is determined by the sum rule

$$\int \rho_{xc}^{\mathrm{WD}}(\mathbf{r}_1, \mathbf{r}_2)\, d\mathbf{r}_2 = \int \rho(\mathbf{r}_2)\bar{h}_0(|\mathbf{r}_1 - \mathbf{r}_2|; \bar{\rho}(\mathbf{r}_1))\, d\mathbf{r}_2 = -1 \tag{8.5.34}$$

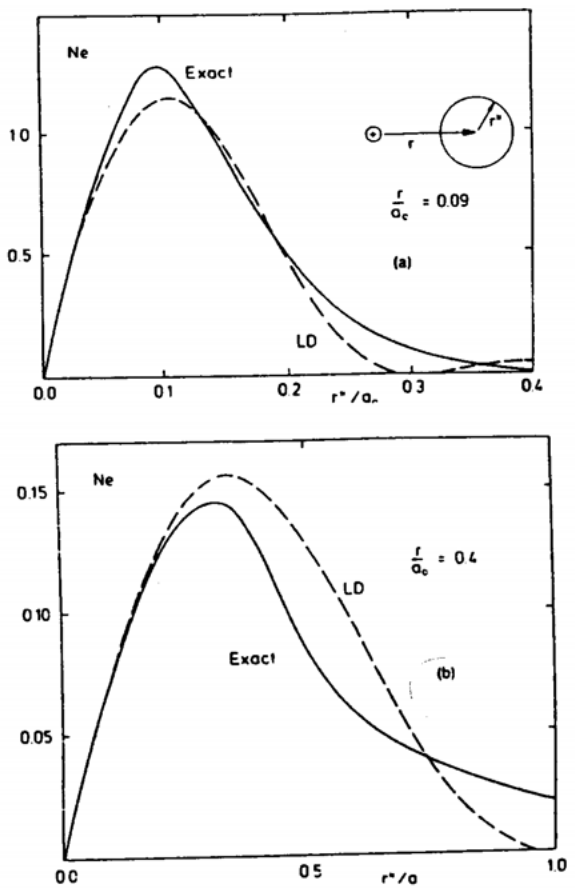

Figure 8.2 Spherical average of the neon atom exchange hole times $\mathbf{r}''$ for (a) $r = 0.09$ a.u. and (b) $r = 0.4$ a.u. The full curves give the exact results and the dashed curves are obtained in the LD approximation. (From Gunnarsson, Jonson, and Lundqvist 1979.)

The WD exchange-correlation energy is given by inserting ρ_{xc}^{WD} into (8.5.12). Comparing (8.5.33) with (8.5.33), we see that ρ_{xc}^{WD} has the correct prefactor $\rho(\mathbf{r}_2)$, which is not the case with ρ_{xc}^{LDA} or ρ_{xc}^{AD}.

The modified WD scheme (MWD) (Gunnarsson and Jones 1980) approximates the pair-correlation function by the approximate analytic function

$$h^{\mathrm{MWD}}(|\mathbf{r}_1 - \mathbf{r}_2|; \rho) = -A \exp\left[-B^5/|\mathbf{r}_1 - \mathbf{r}_2|^5\right] \tag{8.5.35}$$

where the parameters A and B are dependent on ρ and are determined

What about $\epsilon_{xc}^h[\rho]$?

- EXCHANGE: $\epsilon_x^h[\rho] = -\frac{3}{4}\left(\frac{3}{\pi}\right)^{1/3}\rho^{1/3} = -\frac{0.458}{r_s}$ a.u.
  (DIRAC) (2.62)

- CORRELATION: $\epsilon_c^h[\rho] = \begin{cases} \underbrace{A\ln r_s + B + C r_s \ln r_s + D r_s}_{\text{RPA}} & r_s \le 1 \\ \dfrac{\gamma}{(1+\beta_1\sqrt{r_s}+\beta_2 r_s)} & r_s > 1 \end{cases}$
  (PERDEW-ZUNGER) 181 (2.63)

  HIGH DENSITY

  LOW DENSITY

(VOSKO, WILK, NUSAIR '80).

- HIGH-DENSITY: R.P.A. (Gell-Mann-Brueckner '57)
- LOW-DENSITY: Padé fit to Quantum MC results of Ceperley & Alder ('80).

High-density: X dominant, C correction

Low-density: C dominant

Homogeneous electron gas (Fetter & Walecka - Mahan). See

$$E^h[\rho] = \frac{C_k}{r_s^2} - \frac{C_x}{r_s} + C_c \ln r_s + \cdots$$

KINETIC EXCHANGE CORRELATION

$$r_s = \left(\frac{3}{4\pi\rho}\right)^{1/3} \quad \text{or} \quad \rho^{-1} = \frac{4}{3}\pi r_s^3$$

LSDA

Define $\rho_\uparrow(\underline{r})$, $\rho_\downarrow(\underline{r})$ Spin up/down densities.

$$\rho(\underline{r}) = \rho_\uparrow(\underline{r}) + \rho_\downarrow(\underline{r})$$ Charge Density

$$\zeta(\underline{r}) = \frac{\rho_\uparrow(\underline{r}) - \rho_\downarrow(\underline{r})}{\rho(\underline{r})}$$ Magnetization Density.

$E_{ext}[\rho]$, $E_H[\rho]$, $E_{xc}[\rho_\uparrow, \rho_\downarrow]$

$$V_{KS}^{\uparrow}(\underline{r}) = v(\underline{r}) + V_H(\underline{r}) + \frac{\delta E_{xc}}{\delta \rho_\uparrow}$$

$$V_{KS}^{\downarrow}(\underline{r}) = v(\underline{r}) + V_H(\underline{r}) + \frac{\delta E_{xc}}{\delta \rho_\downarrow}$$

$$E_{xc}^{LSDA}[\rho_\uparrow, \rho_\downarrow] = \int [\rho_\uparrow(\underline{r}) + \rho_\downarrow(\underline{r})]\, \varepsilon_{xc}^{h}[\rho_\uparrow, \rho_\downarrow]\, d\underline{r}$$

Obtained interpolating unpolarized → fully pol.
$\zeta = 0$ $\zeta = 1$.

$$\varepsilon_{xc}^{h}[\rho, \zeta] = \varepsilon_{xc}^{h}[\rho, 0] + f(\zeta)\,[\varepsilon_{xc}^{h}[\rho, 1] - \varepsilon_{xc}^{h}[\rho, 0]].$$

$$f(\zeta) = [(1+\zeta)^{4/3} + (1-\zeta)^{4/3} - 2]/(2^{4/3} - 2)$$

LDA-LSDA TRENDS

1. FAVOURS MORE HOMOGENEOUS e-DENSITIES
2. OVERBINDS MOLECULES AND SOLIDS (HF UNDERBINDS)
3. GEOMETRIES, BOND LENGTHS AND ANGLES; VIBRATIONAL FREQUENCIES $\lesssim$ 2-3%.
4. DIELECTRIC CONST. OVERESTIMATED $\sim$10%
5. BOND LENGTHS TOO SHORT FOR WEAKLY BOUND SYSTEMS (H-BOND _ VDW)
6. CORRECT CHEMICAL TRENDS (E_I)

LIMITATIONS

1. (ATOMIC) CORE ELECTRONS POORLY DESCRIBED (HF MUCH BETTER)
2. XC POTENTIAL DECAYS EXPONENTIALLY INTO VACUUM, RATHER THAN $-e^2/r$. $\Rightarrow$ WRONG DISSOCIATION + IONIZATION.
3. METALLIC SURFACES AND PHYSISORPTION.
4. NEGATIVELY CHARGED IONS (sic)
5. WEAKLY BOUND SYSTEMS $<$ H-BONDS (?!) VDW (semi-local!)
6. BAND GAP IN SEMICONDUCTORS ($<$ 40%)
7. STRONGLY CORRELATED SYSTEMS (OXIDES - UO_2)

Atomic Ionization Energies

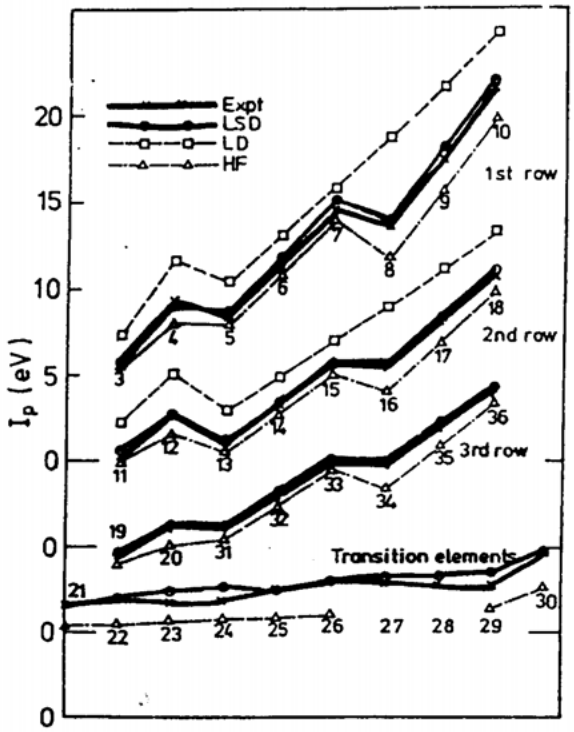

FIG. 8. First ionization energy of atoms in the local-density (LD), local spin-density (LSD), and Hartree-Fock (HF) approximations compared with experiment. The numbers show the atomic numbers of the atoms considered. For reasons of clarity, the zero of energy is shifted by 5, 10, and 15 eV for the second row, the third row, and the transition-element row, respectively. The LD results for the first and second rows are increased by an additional 2 eV.

R.O. Jones and O. Gunnarsson
Rev. Mod. Phys., Vol. 61, No. 3, July 1989

	I^{exp}	$I^{LSD-\Delta SCF}$	$I^{LSD-\nu}$ [eV]
Li	5.4	5.7	3.4
Be	9.3	9.1	5.7
B	8.3	8.8	4.2
C	11.3	12.1	6.3
N	14.5	15.3	6.5
O	13.6	14.2	7.4
F	17.4	18.4	10.5
Ne	21.6	22.6	13.3

BEYOND LDA

- INHOMOGENEITIES IN ρ
- SELF-INTERACTION CANCELLATION
- NON-LOCALITY IN XC.
- STRONG LOCAL CORRELATIONS.

- GRADIENT EXPANSIONS
- WEIGTHED DENSITY
- EXACT EXCHANGE (OEP)
- HYBRIDS DFT-HF
- VAN DER WAALS FUNCTIONALS
- LDA +U
- GW APPROXIMATION
- SiC

GRADIENT EXPANSION

$$E_{xc}[\rho] = \int \underbrace{A_{xc}[\rho]}_{\text{LDA}} \rho^{4/3}(r)\, dr + \underbrace{\int C_{xc}[\rho] \frac{|\nabla \rho|^2}{\rho^{4/3}} dr}_{\text{correction for inhomogeneous systems}} + \dots \qquad (2.65)$$

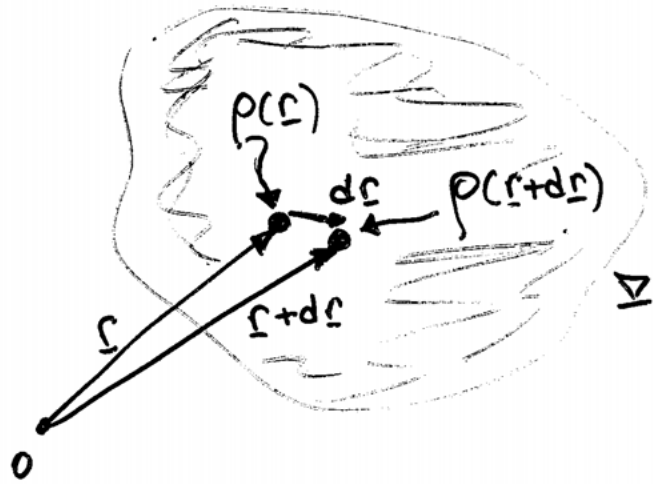

$$\nabla\rho = \left[\frac{\rho(r+dr) - \rho(r)}{dr}\right] \cdot \hat{u}$$

In the gradient expansion, $\nabla\rho$ enters in absolute value, the direction being absent.

WARNINGS

1) THIS EXPANSION IS NOT MONOTONICALLY CONVERGENT

2) HIGHER ORDER TERMS ARE DIVERGENT, AND BECOME FINITE ONLY AFTER BEING RESUMMED TO INFINITE ORDER (Resummation)

3) DOESN'T SATISFY SUM RULES!!

The expression above, however, should be recovered for slowly varying densities.

Langreth-Mehl ('81-'83)

Most of the problem comes from Correlation - Real space cutoff method eliminates divergencies and enforces some limits (known)

$$\epsilon_c = \epsilon_c^{RPA} + a \frac{|\nabla\rho|^2}{\rho^{4/3}} \cdot \left(2e^{-F} + \underbrace{18 f^2}_{\text{cancelled by exchange.}}\right)$$

$$F = b \frac{|\nabla\rho|}{\rho^{7/6}} \quad \text{(cutoff)}$$

+ CORRECT scaling behaviour in the high density limit.
- RPA instead of LDA for ϵ_c
- Does not recover GEA.

Perdew ('85)

Enforcing exactly known properties of the X and C holes IMPROVES the quality of the funct.

Perdew-Wang ('86)

$$\epsilon_c = \epsilon_c^{LDA} + e^{-\Phi} C_c(\rho) \frac{|\nabla\rho|^2}{\rho^{4/3}}$$

$$\Phi = 1.745 \hat{f} \frac{C_c(\infty)}{C_c(\rho)} \frac{|\nabla\rho|}{\rho^{7/6}} \quad \text{Langreth-Mehl-like}$$

$$C_c(\rho) = C_1 + \frac{C_2 + C_3 r_s + C_4 r_s^2}{1 + C_5 r_s + C_6 r_s^2 + C_7 r_s^3}$$

beyond RPA coeff. (Rasolt & Geldart) (Hu & Langreth)

- Correct LDA limit for uniform density.
- Recovers gradient expansion for slowly varying densities

$$\epsilon_x = \epsilon_x^{LDA}\left(1 + 0.0864\frac{s^2}{m} + bs^4 + cs^6\right)^m$$

NOT FITTED TO DATA.

$$m = \frac{1}{15}\,, \quad s = \frac{|\nabla\rho|}{2k_F\rho}\,; \quad k_F = 3\pi^2\rho^{1/3}$$

s: scaled density

- $\rho_x(\underline{r},\underline{r}') \le 0$
- $\int \rho_x(\underline{r},\underline{r}')\,d\underline{r}' = -1$

correct LDA limit.

Becke ('88)

$$\epsilon_x = \epsilon_x^{LDA}\left(1 - \frac{\beta}{2^{1/3}A_x}\cdot\frac{x^2}{1+6\beta x\sinh^{-1}(x)}\right)$$

$$x = 2^{1/3}\frac{|\nabla\rho|}{\rho^{4/3}}\,; \quad A_x = \frac{3}{4}\left(\frac{3}{\pi}\right)^{1/3}\,; \quad \boxed{\beta = 0.0042}$$

FITTED TO MOLECULAR DATA.

- Correct asymptotic behaviour of $v_x(\underline{r}) \xrightarrow[r\to\infty]{} -1/r$.

AB INITIO vs. AB FINE

Perdew-Wang ('91)

+ Scaling limits like $\lim_{\lambda\to 0}\frac{1}{\lambda}E_{xc}[\rho(x,y,z)] = 0$

Lee-Yang-Parr ('88) — BLYP

$$\epsilon_c = -a\frac{1}{1+d\rho^{-1/3}}\left\{\rho + b\rho^{-2/3}\left[C_F\rho^{5/3} - 2t_W + \frac{1}{9}\left(t_W + \frac{\nabla^2\rho}{2}\right)\right]e^{-c\rho^{-1/3}}\right\}$$

$$t_W = \frac{1}{8}\left(\frac{|\nabla\rho|^2}{\rho} - \nabla^2\rho\right)$$

- from Colle-Salvetti ϵ_c for He.
- No LDA limit.

Perdew-Burke-Ernzerhof (PBE): the ultimate GGA. ('96)

LSDA + energetically most important features

$$E_{xc}[\rho] = \int \rho(\underline{r})\, \epsilon_{xc}^{LDA}[\rho]\, \underbrace{F_{xc}(\rho, \zeta, s)}_{\text{enhancement factor}}\, d\underline{r}$$

ρ = density
ζ = spin polarization
$s = |\nabla\rho|/2k_F\rho$ density gradient.

Exchange:

$$F_x(s) = 1 + \kappa - \frac{\kappa}{1 + \mu s^2/\kappa}$$

- Uniform scaling
- LDA limit
- Spin-scaling relationship
- LSDA linear response
- Lieb-Oxford bound $E_x \geq -1.68\,\rho^{4/3}$ ($\kappa < 0.8$)

→ interpolates between LDA and full GGA.

[Can play with κ and μ...]

Correlation:

$$E_c^{GGA} = \int \rho(r)\left[\epsilon_c^{LDA}(\rho,\zeta) + H[\rho,\zeta,t]\right] d\underline{r}$$

$$H[\rho,\zeta,t] = \gamma\phi^3 \ln\left\{1 + \frac{\beta}{\gamma}t^2\left[\frac{1+At^2}{1+At^2+A^2t^4}\right]\right\}$$

with $t = |\underline{\nabla}\rho|/2\phi k_s\rho$; $k_s = k_{TF}$ (Thomas-Fermi)

$$\begin{cases} \phi(\zeta) = [(1+\zeta)^{2/3} + (1-\zeta)^{2/3}]/2 \\ A = \frac{\beta}{\gamma}\left[e^{-\epsilon_c^{LDA}/\gamma\phi^3} - 1\right]^{-1} \end{cases}$$

- Correct second order expansion for $t \to 0$
- Enforces the correlation hole sum rule
- $\epsilon_c[\rho]$ vanishes for rapidly varying densities
- Cancels the logarithmic singularity of ϵ_c^{LDA} in the high-density limit (uniform scaling)

Sacrifices ~~a~~ for ~~less~~ important features.

PROPERTIES of GGA.

- Improves atomization & surface energies
- Favours density inhomogeneities
- Increases lattice constants of metals
- Favours non-spherical distortions BECKE.
- Improves bond lengths
- Improves energetics, geometry & dyn of weakly bound systems (H-bonds).
- Still incorrect asymptotic decay into vacuum.
  $v_{xc}(r) \longrightarrow -\exp(-\alpha r)$ in the vacuum.
  ($-1/r$ is correct.)
- Some improvement for the gap problem
- What's correct in LDA, is worsened by GGA.

- No derivative discontinuities
  (incorrect dissociation limit → fractionally charged frag.)
- Intraconfigurational (interterm) errors of ionization potentials & e^- affinities.

- As in the LDA, in GGA there is still an error cancellation between X and C.
- This cancellation is not complete in the long-range part ⇒ exp vs $1/r$ decay.
- X hole is more long-ranged than XC hole.

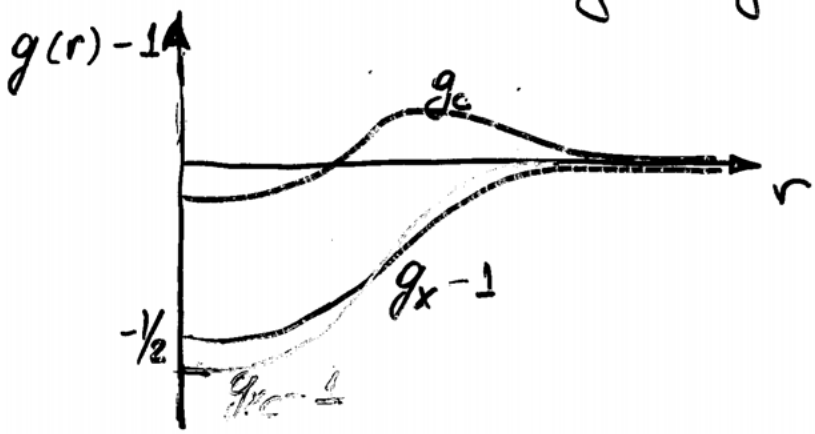

EXCHANGE LIMITS ACCUR. OF GGA

HYBRID FUNCTIONALS

G. SCUSERIA

$$E_{XC}[\rho,\{\varphi\}] = \underset{\uparrow}{\alpha} E_X^{GGA} + (1-\alpha) E_X^{HF} + E_C^{GGA}$$

~ 0.75

B3LYP ≳ MP2 quality

Again ... ab fine. Very popular in chemistry.

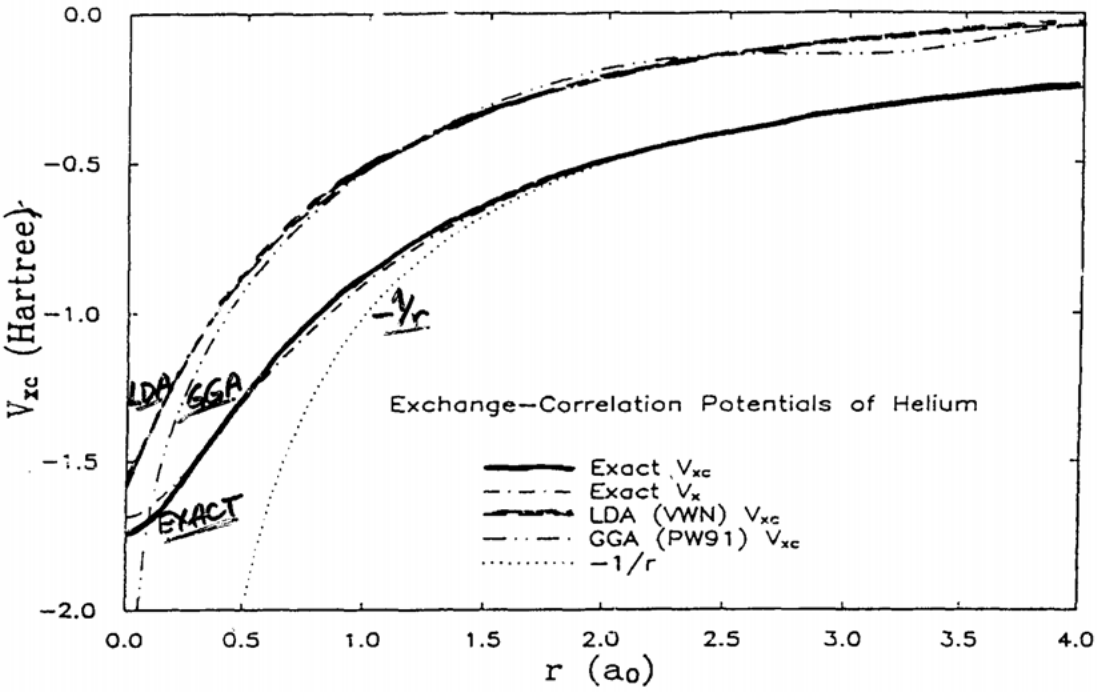

FIG. 3. Comparison of the LDA. and GGA v_{xc} with the exact v_{xc} and with v_x for He.

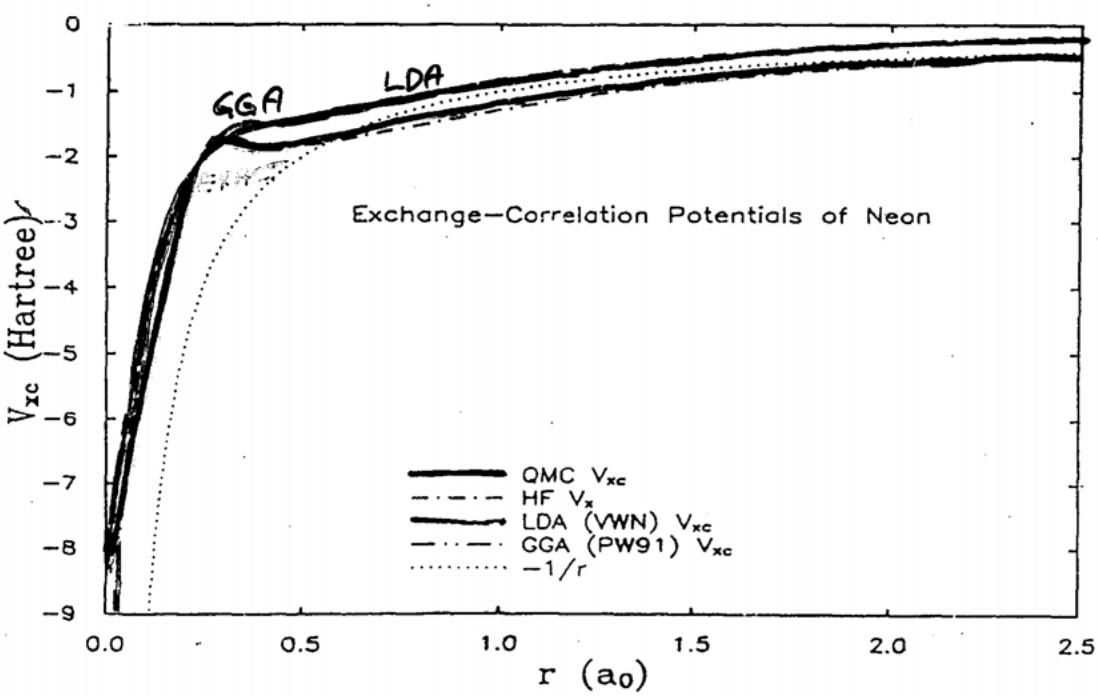

FIG. 4. Comparison of the LDA, and GGA v_{xc} with an accurate v_{xc} and with v_x for Ne.

C.J. Umrigar, X. Gonze

Conference on Concurrent Computing in the Physical Sciences 198?

Phys. Rev. A 50 3827 (1994)

II. ATOMS

As a first test of our density functionals, we consider the total and electron-removal energies of atoms. The electron density may be constructed via self-consistent solution of either the Hartree-Fock (HF) or Kohn-Sham equations. The former approach, which we adopt here, has certain advantages: Its one-electron potential has the correct asymptotic ($r \to \infty$) limit[30,39] (so that negative-ion solutions exist), and the exact exchange energy E_x^{HF} is evaluated automatically. For a given continuum density-functional approximation, there is some energy difference between the HF and Kohn-Sham densities. For Zn, this difference is about 1 eV in the total energy and about 0.2 eV in the ionization energy. (Full density-functional self-consistency lowers the energy of the neutral atom more than that of the positive ion; compare Table III of Ref. 13 to our Table II.) From the discussion of Sec. I, we expect that the Hartree-Fock density is more realistic and thus more appropriate for comparison with experiment.

Following the approach of Lagowski and Vosko,[11] we have performed self-consistent spin-restricted Hartree-Fock calculations in the central-field approximation for the atoms with $1 \le Z \le 30$ and their first positive and negative ions. Each atom or ion is assigned its observed ground-state configuration and term.[44,45] The nonspherical density is constructed by occupying nonrelativistic spherical-harmonic orbitals in a Slater determinant with $M_L = L$ and $M_S = S$. The scalar-relativistic correction to the total energy is treated as a first-order perturbation.

Table I shows $-E_x^{HF}$, the magnitude of the exact or Hartree-Fock exchange energy, as well as the difference $-E_{xc}^{DF} + E_x^{HF}$, whose experimental value[11] is the magnitude of the correlation energy. The first density-functional (DF) considered is PW GGA-IIX, the exchange-energy functional of Eqs. (3)–(8). The PW GGA-IIX column of Table I shows an error relative to HF that is typically only a fraction of 1% of the exact exchange energy, as expected.[7,10] The other density functionals considered are the LSD, PW GGA-I, PW GGA-II, and PW GGA-IIA approximations for the exchange-correlation energy, as defined in Sec. I. All take $\varepsilon_c(r_s,\zeta)$ from Ref. 26, except PW GGA-I which employs Ref. 39. Clearly the large total-energy errors of LSD and HF, which are significantly reduced by PW GGA-I[7,8,11–13] are further reduced by PW GGA-II and PW GGA-IIA. The LSD overestimation of the magnitude of the correla-

TABLE II. First ionization energies (I) of 30 atoms. All calculations employ Hartree-Fock densities for the observed ground-state configuration and term of the neutral atom and positive ion, and include scalar relativity as a perturbation. Experimental values from Ref. 44.

		I (eV)						
Atom	Process	HF	PW GGA-IIX	LSD	PW GGA-I	PW GGA-II	PW GGA-IIA	Expt.
H	*s*	13.61	13.45	13.00	13.65	13.63	13.63[a]	13.61
He	*s*	23.45	23.51	24.27	24.96	24.56	24.56[a]	24.59
Li	*s*	5.34	5.42	5.45	5.63	5.61	5.55	5.39
Be	*s*	8.05	8.17	9.01	9.22	9.04	9.14	9.32
B	*p*	7.93	7.92	8.57	8.69	8.57	8.53	8.30
C	*p*	10.78	10.95	11.67	11.65	11.64	11.56	11.26
N	*p*	13.95	14.20	14.92	14.84	14.91	14.82	14.53
O	*p*	11.88	12.38	13.82	14.12	13.76	13.90	13.62
F	*p*	15.70	16.53	17.94	17.94	17.79	17.87	17.42
Ne	*p*	19.82	20.77	22.10	21.99	21.96	21.99	21.56
Na	*s*	4.96	5.19	5.31	5.45	5.36	5.26	5.14
Mg	*s*	6.62	6.89	7.70	7.89	7.64	7.81	7.65
Al	*p*	5.49	5.38	5.98	6.06	6.01	5.95	5.99
Si	*p*	7.64	7.59	8.21	8.25	8.25	8.19	8.15
P	*p*	10.03	9.88	10.51	10.54	10.56	10.51	10.49
S	*p*	9.01	9.07	10.49	10.50	10.30	10.44	10.36
Cl	*p*	11.78	11.88	13.18	13.14	13.05	13.11	12.97
Ar	*p*	14.75	14.71	15.92	15.89	15.85	15.86	15.76
K	*s*	4.02	4.28	4.48	4.60	4.46	4.36	4.34
Ca	*s*	5.14	5.44	6.20	6.36	6.10	6.26	6.11
Sc	*s*	5.38	5.71	6.56	6.73	6.42	6.66	6.54
Ti	*s*	5.54	5.88	6.79	6.97	6.62	6.91	6.82
V	*sd*	6.06	5.76	6.17	6.60	5.96	6.33	6.74
Cr	*s*	6.00	7.06	7.36	7.45	7.23	7.20	6.77
Mn	*s*	5.94	6.29	7.31	7.50	7.06	7.50	7.43
Fe	*s*	6.34	6.84	7.85	8.04	7.59	7.95	7.87
Co	*sd*	8.21	7.57	7.56	8.01	7.47	7.45	7.86
Ni	*sd*	8.11	7.05	7.12	7.62	7.00	6.99	7.63
Cu	*s*	6.56	7.65	8.16	8.32	8.01	7.86	7.73
Zn	*s*	7.78	8.71	9.64	9.82	9.40	9.61	9.39

[a]Value identically the same as with PW GGA-II.

ENHANCEMENT FACTORS

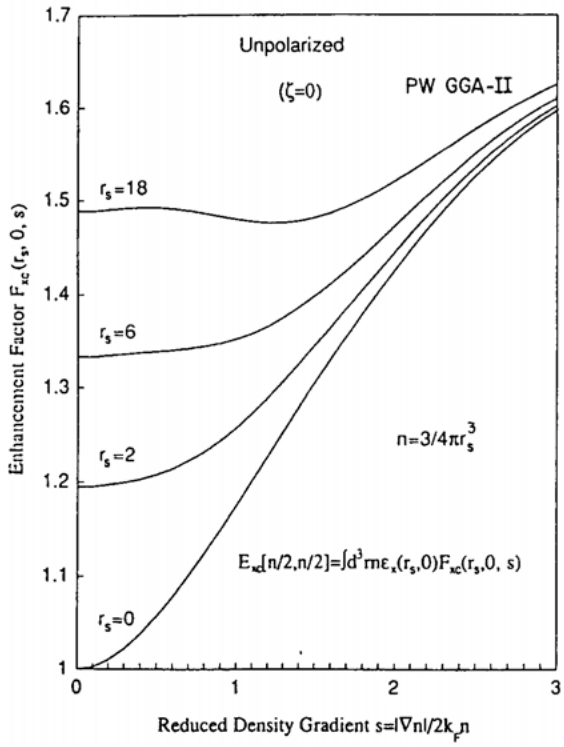

FIG. 3. PW GGA-II nonlocality in the spin-unpolarized case. The enhancement factor $F_{xc}(r_s,0,s)$ (relative to spin-unpolarized local exchange) is plotted vs the reduced density gradient s for several values of the local-density parameter r_s. The corresponding enhancement factors for LSD are the horizontal lines $F_{xc}(r_s,0,0)=\varepsilon_{xc}(r_s,0)/\varepsilon_x(r_s,0)$. For the second-order gradient expansion, they are downward-turning parabolas $F_{xc}(r_s,0,0)-|C(r_s,0)|s^2$.

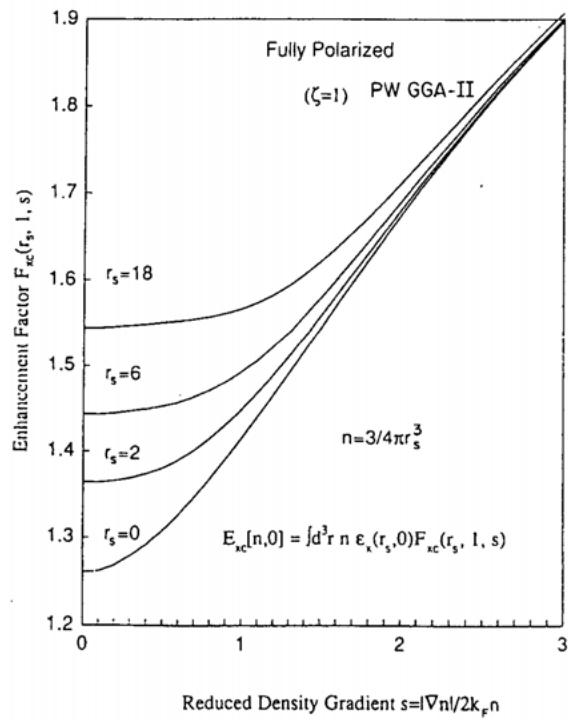

FIG. 4. Same as Fig. 3, but for the fully spin-polarized case.

The values of s that are important in the interior of a metal typically fall in the range $0 \lesssim s \lesssim 2.0$. Atoms sample the range $0.2 \lesssim s$, with s diverging into the vacuum around the atom.[72] (Within an electronic shell, $|\nabla n|/n$ is approximately constant, but k_F^{-1} and s increase in the outward direction.) Clearly, for most physical properties of real systems, the nonlocal effect of PW GGA-II is *opposite* to that of the second-order gradient expansion. Thus, Bagno, Jepsen and Gunnarsson[21] found that the gradient expansion shrinks the lattice constants of metals, which are already too small in LSD, and further destabilizes the bcc ferromagnetic ground state of Fe, which is wrongly unstable in LSD. PW GGA-II has the opposite (and correct) effects.

The exchange-only PW GGA-IIX nonlocality is presented in the $r_s=0$ curves of Figs. 3 and 4. The nonlocality of exchange ($E_x^{\text{PW GGA-II}} < E_x^{\text{LSD}} < 0$), which favors density inhomogeneity, is strong when s is of order unity, i.e., when the density varies significantly over the range of the exchange hole. An opposite nonlocality ($0 > E_c^{\text{PW GGA-II}} > E_c^{\text{LSD}}$), which opposes density inhomogeneity, extinguishes the correlation contribution to F_{xc} as $t \to \infty$. (Compare the similar behavior of the linear response function in Ref. 41, and the somewhat different behavior produced by the wave-vector-space cutoff of Refs. 4 or 8.) In the high-density limit ($r_s \to 0$), the correlation contribution vanishes on the scale of these figures. But for metallic densities ($2 \lesssim r_s \lesssim 6$), the nonlocality of correlation cancels much of that for exchange ($E_{xc}^{\text{PW GGA-II}} \lesssim E_{xc}^{\text{LSD}}$). For these and lower densities, the exchange-correlation hole is significantly deeper and (apart from oscillations) more short ranged than the exchange hole, making F_{xc} larger and more "local" than F_x. As a result, LSD can give a reasonably good description of valence-electron energies in metals, even though it makes serious errors for the cores.

Since the residue of this cancellation between nonlocalities is still exchangelike in PW GGA-II, the principal PW GGA-II nonlocal effect is to favor density inhomogeneity or surface formation more than LSD does. Thus the PW GGA-II correction to LSD lowers total, atomization, surface, and curvature energies. It enlarges the lattice constants of metals, where expansion continuously increases the inhomogeneity. PW GGA-II also favors nonspherical distortions over spherical densities.

Although the PW GGA-II functional improves upon LSD, too much should not be expected from it:

(1) Even the exact density functional would not predict all excited-state energies,[1,2] nor would its Kohn-Sham eigenvalue spectrum predict the fundamental gap (twice "hardness") of an insulator or semiconductor[28,29] or the exact Fermi surface of a metal.[92]

(2) Many incorrect features of LSD are carried over into PW GGA-II and other GGA's: (a) Incorrect asymptotic decay[30,39] of the density and one-electron potential into the vacuum, blocking self-consistent solutions for negative ions; (b) absence of derivative discontinuities, leading to incorrect fractionally charged fragments instead of neutral atoms as dissociation products of heteronuclear molecules or solids;[28,29] (c) interconfigurational and interterm errors of ionization energies and

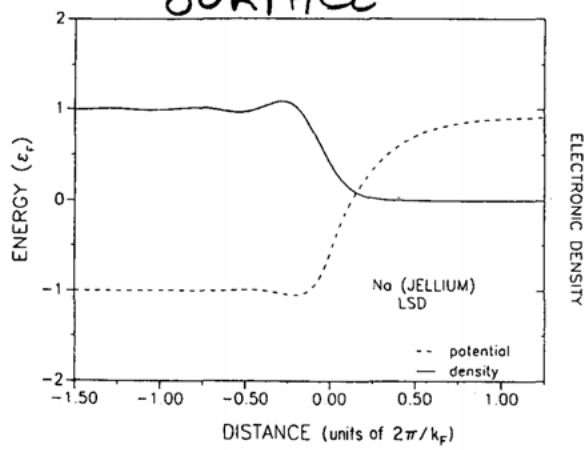

FIG. 1. LSD solution for the $r_s=3.99$ jellium surface. The solid curve is the electron-density profile, measured in units of the bulk density $k_F^3/3\pi^2$. The dashed curve is the self-consistent one-electron potential, measured in units of the bulk Fermi energy $k_F^2/2$. A constant has been added to this potential to make it tend to $-k_F^2/2$ in the bulk. Distance from the jellium edge is measured in units of the Fermi wavelength $2\pi/k_F$.

with PW GGA-II correlation.)

The correction that we find to the LSD surface energy is rather small, as a result of a delicate cancellation between the nonlocalities of exchange and correlation (Tables X–XII). This correction is much smaller than that found by the Fermi hypernetted-chain method,[85] which was regarded as the standard before the advent of the quantum Monte Carlo calculation.[81] However, it is consistent with the results of Skriver and Rosengaard,[86] who calculated LSD surface energies, for the close-packed faces of the alkali metals, that agree closely with measured liquid-metal surface tensions extrapolated to zero temperature. Note further that a sophisticated version of the fully nonlocal weighted-density approximation gives surface energies close to those of LSD.[87]

The LSD and PW GGA-II electron-density profiles

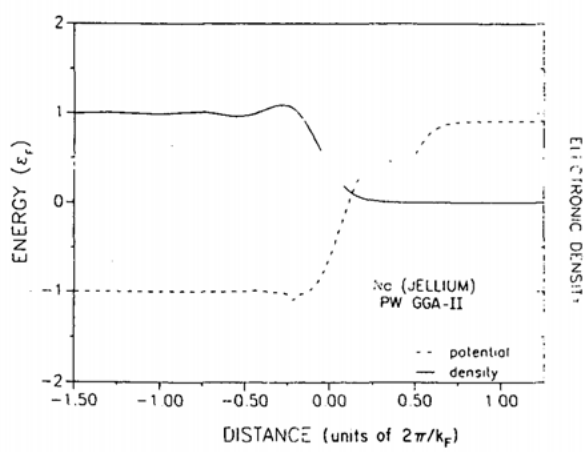

FIG. 2. PW GGA-II solution for the $r_s=3.99$ jellium surface. See caption of Fig. 1.

and one-electron potentials for the $r_s=3.99$ jellium surface are displayed in Figs. 1 and 2. On the scale of these figures, the LSD and PW GGA-II density profiles are indistinguishable. The potentials are barely distinguishable until the electron density has decayed to about 10% of its bulk value. From this point, the PW GGA-II potential first rises above and then dips below the LSD potential. A similar oscillation is found in the PW GGA-I and LM potentials for atoms.[19]

VI. ATOMS, SOLIDS, AND SURFACES IN THE JELLIUM MODEL: A UNIFIED PERSPECTIVE

Here we present simple estimates which tie together our results for atomic total energies (Sec. II), atomization energies (Sec. III), and surface and curvature energies (Sec. V). Use will be made of the jellium model of Sec. V.

According to the liquid-drop model for crystalline metals,[84] the expansion (22) can be valid even for microscopic radii of curvature, so long as electronic shell-structure effects may be neglected. Clear-cut examples are provided by the monovacancy-formation energy and the crystal-face dependence of the surface energy for a metal of infinite volume. The expansion (22) also seems to apply to one-electron atoms, i.e., the shell-structure oscillation tends to vanish for these systems with half-filled shells.

Consider a monovalent atom of jellium, i.e., one electron bound to a uniform positive background of density $3/4\pi r_s^3$ confined inside a sharp spherical surface of radius r_s. The total energy is[88] $-I+3/5r_s$, where I is the energy needed to ionize the electron and $3/5r_s$ is the electrostatic energy of the positive background. Since this is a one-electron problem, I is easily calculated exactly or in a density-functional approximation.[88]

The cohesive energy of jellium is the atomization energy per atom, i.e.,

$$\epsilon_{coh}=[-I+3/5r_s]-\epsilon\ , \tag{25}$$

where $\epsilon=3k_F^2/10+\epsilon_{xc}(r_s)$ is the energy per electron in the uniform or condensed phase. By Eq. (22), the liquid-drop-model estimate of the cohesive energy[84] is just the energy needed to create the curved surface of the jellium atom:

$$\sigma 4\pi r_s^2+\gamma 2\pi r_s\ . \tag{26}$$

In Table XIII we compare the LSD cohesive energy of Eq. (25) against the liquid-drop prediction of Eq. (26), using LSD values for σ and γ from Sec. V. We also compare the exact cohesive energy against the liquid-drop prediction, using PW GGA-II values for σ and γ. [We omit the long-range contribution of Eq. (24), which arises from an effect present only for a semi-infinite system and thus irrelevant to the cohesive energy.] The following conclusions may be drawn: (1) Except at the highest density considered ($r_s=2.07$), the liquid-drop model has good quantitative accuracy. Even at $r_s=2.07$, the curvature term helps. (The liquid-drop model must fail in the limit $r_s\to 0$, in which the jellium atom reduces to hydro-

Meta GGA

Gross & Dreizler ('81) + Perdew ('85) + Ghosh & Parr ('86)

$$F_X(p,q) = 1 + \frac{10}{81}p + \frac{146}{2025}q^2 - \frac{73}{405}qp + Dp^2 + \dots \quad (2.67)$$

$$p = \frac{|\nabla\rho|}{\rho^{8/3}} \cdot (C_p) \qquad \text{(Gradient)}^2$$

$$q = \frac{\nabla^2\rho}{\rho^{5/3}} \cdot (C_q) \qquad \text{(Laplacian)}$$

Perdew-Kurth-Zupan-Blaha (PKZB) ('99) (TPSS)

Exchange

$$F_X^{MGGA}(p,\bar{q}) = 1 + K - \frac{K}{1 + x/K} \quad (2.68)$$

→ PBE-like.

$$x = x(p,\bar{q}) = \frac{10}{81}p + \frac{146}{2025}\bar{q}^2 - \frac{73}{405}\bar{q}p + \left(D + \frac{1}{K}\left(\frac{10}{81}\right)^2\right)p^2$$

$$\bar{q} = C_q\left(\frac{\tau}{\rho^{5/3}} - \frac{q}{20} - \frac{p}{12}\right) \longrightarrow q \quad \text{slowly varying densities}$$

$$\left[\tau = \frac{1}{2}\sum_{\alpha=1}^{occ} |\nabla\varphi_\alpha(\vec{r})|^2 \quad \text{kinetic energy density}\right]$$

2nd order gradient expansion:

$$\tau^{GEA} = \frac{3}{10}(3\pi^2)^{2/3}\rho^{5/3} + \frac{1}{72}\frac{|\nabla\rho|^2}{\rho} + \frac{1}{6}\nabla^2\rho$$

- spin-scaling relation
- uniform-density scaling relation
- Lieb-Oxford bound on X.
- D fitted to molecular atomization energies
- Correct linear response to 4th order in $k/2k_F$.
  (PBE recovers LSDA linear response)

Correlation:

$$E_c^{MGGA} = \int \rho(\underline{r}) \underbrace{\varepsilon_c^{GGA}}_{PBE}(\rho_\uparrow, \rho_\downarrow, \nabla\rho_\uparrow, \nabla\rho_\downarrow) \cdot \left[1 + C\left(\frac{\sum_\sigma \tau_\sigma^W}{\sum_\sigma \tau_\sigma}\right)^2\right] d\underline{r}$$

$$-(1+C)\sum_\sigma \int \left(\frac{\tau_\sigma^W}{\tau_\sigma}\right)^2 \rho_\sigma(\underline{r}) \underbrace{\varepsilon_c^{GGA}}_{PBE}(\rho_\sigma, 0, \nabla\rho_\sigma, 0)\, d\underline{r}$$

$$\tau_\sigma^W = \frac{1}{8} \frac{|\nabla\rho_\sigma|^2}{\rho_\sigma}$$ von Weizsäcker K.E. density

- τ_σ^W is exact for a one-electron system.
  $\Rightarrow E_c^{MGGA} = 0$ for a one-electron system !! (SIC)

- for many-electron systems, the SIC is not complete but it's shifted to 4th order in $\nabla\rho \Rightarrow$ OK for slowly varying densities.
- C fitted to surface correlation energies for jellium.

Hence: $E_c(N_e) = \begin{cases} \dots \\ \dots \\ \dots \end{cases} \longrightarrow$ correct.

META-GGA

$(\nabla\rho, \nabla^2\rho)$

Perdew, Kurth, Zupan & Blaha

PRL 82, 2544 ('99)

TABLE I. Atomization energies (in kcal/mole). All functionals evaluated on GGA densities at experimental geometries. Zero-point vibration removed from experimental energies [5]. The GGA is PBE [5], and the LSD is the local part of PBE. The Gaussian basis sets are of triple-zeta quality, with p and d polarization functions for H and d and f polarization functions for first- and second-row atoms.

Molecule	ΔE^{LSD}	ΔE^{GGA}	ΔE^{MGGA}	ΔE^{expt}
H_2	113.3	104.6	114.5	109.5
LiH	61.1	53.5	58.4	57.8
CH_4	462.6	419.8	421.1	419.3
NH_3	337.3	301.7	298.8	297.4
OH	124.2	109.8	107.8	106.4
H_2O	266.6	234.2	230.1	232.2
HF	162.3	142.0	138.7	140.8
Li_2	23.8	19.9	22.5	24.4
LiF	156.1	138.6	128.0	138.9
Be_2	12.8	9.8	4.5	3.0
C_2H_2	460.3	414.9	401.2	405.4
C_2H_4	632.7	571.5	561.5	562.6
HCN	360.8	326.1	311.8	311.9
CO	298.9	268.8	256.0	259.3
N_2	266.9	243.2	229.2	228.5
NO	198.4	171.9	158.5	152.9
O_2	174.9	143.7	131.4	120.5
F_2	78.2	53.4	43.2	38.5
P_2	143.0	121.1	117.8	117.3
Cl_2	82.9	65.1	59.4	58.0
Mean abs. error	31.69	7.85	3.06	...

TABLE II. Exchange and correlation contributions to surface energies (in erg/cm^2) for jellium, using self-consistent LSD densities. Exact surface exchange energies were provided by Pitarke and Eguiluz [29].

r_s	σ_x^{exact}	σ_x^{LSD}	σ_x^{GGA}	σ_x^{MGGA}	σ_c^{LSD}	σ_c^{GGA}	σ_c^{MGGA}
2.00	2624	3037	2438	2578	317	827	824
2.07	2296	2674	2127	2252	287	754	750
2.30	1521	1809	1395	1484	210	567	564
2.66	854	1051	770	825	137	382	380
3.00	526	669	468	505	95	275	274
3.28	364	477	318	346	72	215	214
4.00	157	222	128	142	39	124	124
5.00	57	92	40	47	19	67	66
6.00	22	43	12	15	10	40	40

TABLE III. Lattice constants (in Å) for some solids studied in Ref. [32], from scalar-relativistic all-electron full-potential linearized augmented plane wave calculations [33] without zero-point anharmonic expansion. GGA densities used for all but the LSD calculations.

Solid	a^{LSD}	a^{GGA}	a^{MGGA}	a^{expt}
Na	4.05	4.20	4.31	4.23
NaCl	5.47	5.70	5.60	5.64
Al	3.98	4.05	4.02	4.05
Si	5.40	5.47	5.46	5.43
Ge	5.63	5.78	5.73	5.66
GaAs	5.61	5.76	5.72	5.65
Cu	3.52	3.63	3.60	3.60
W	3.14	3.18	3.17	3.16
Mean abs. error	0.078	0.051	0.059	...

← erratum

SIC (PERDEW-ZUNGER)

self-interaction can be removed at the level of classical electrostatics.

$$E_H = \frac{1}{2}\iint \frac{\rho(\underline{r})\,\rho(\underline{r}')}{|\underline{r}-\underline{r}'|}\,d\underline{r}\,d\underline{r}'$$

$$E_{SIC} = E_H - \frac{1}{2}\sum_{i=1}^{N_{occ}} \frac{|\varphi_i(\underline{r})|^2\,|\varphi_i(\underline{r}')|^2}{|\underline{r}-\underline{r}'|}$$

$$\Rightarrow\quad v_{SIC}^{(i)}(\underline{r}) = v_H(\underline{r}) - \int \frac{|\varphi_i(\underline{r}')|^2}{|\underline{r}-\underline{r}'|}\,d\underline{r}'$$

- POTENTIAL DEPENDS ON STATE (i).

$$\left(-\frac{\hbar^2}{2m}\nabla^2 + v_{SIC}^{(i)} + v_{ext} + \mu_{xc}\right)\varphi_i = \varepsilon_i\varphi_i$$

- NOT AN EIGENVALUE PROBLEM ANY MORE.
- φ_i ORTHOG. NOT GUARANTEED, BUT CAN BE IMPOSED.
- SIMILAR TO HARTREE-FOCK, BUT MB-WFN NOT INVARIANT AGAINST ORBITAL TRANSF.
- RESULT NOT UNIQUE. DEPENDS ON CHOICE OF φ_i. (UNITARY ... LOCALIZATION ...)

VAN DER WAALS

DYNAMICAL CORRELATION EFFECT (NON-LOCAL)

$\Delta n_1(\vec{r},t) \longrightarrow \underline{E}_1(\vec{r},t) \cdot \Delta n_2(\vec{r},t)$

DIPOLAR FIELD — DIPOLE

DIPOLE-DIPOLE INTERACTION DUE TO QUANTUM FLUCTUATIONS OF DENSITY.

FUNCTIONAL (DION et al. 2006)

$$E_{VDW} = \iint \rho(\vec{r})\,\boxed{\phi(\vec{r},\vec{r}')}\,\rho(\vec{r}')\,d\vec{r}\,d\vec{r}'$$

VDW KERNEL

$\phi(\vec{r},\vec{r}')$ DEPENDS ON $\rho(\vec{r})$ AND $\rho(\vec{r}') \Rightarrow$ FULLY NON-LOCAL.

- EXPENSIVE DOUBLE INTEGRAL
- EFFICIENT IMPLEMENTATION (Soler 2009)

$\phi(\vec{r},\vec{r}')$: GOOD APPROXIMATIONS BASED ON DYNAMICAL RESPONSE THEORY.

LDA + U

- STRONG ONSITE CORRELATIONS ARE NOT CAPTURED BY LDA/GGA.
- IMPORTANT FOR LOCALIZED d AND f BANDS, WHERE MANY ELECTRONS SHARE THE SAME SPATIAL REGION (SELF-INTERACTION PROBLEM).

SOLUTION (SEMI-EMPIRICAL): SEPARATE OCCUPIED AND EMPTY STATES BY AN ADDITIONAL ENERGY U AS IN HUBBARD'S MODEL.

$$E_{LDA+U} = E_{LDA} - \frac{1}{2} U N(N-1) + \frac{1}{2} U \sum_{i \neq j} f_i f_j$$

f_i = ORBITAL occupations.

SHIFT IN EIGENVALUES:

$$\varepsilon_i = \frac{\partial E_{LDA+U}}{\partial f_i} = \varepsilon_i^{LDA} + U\left(\frac{1}{2} - f_i\right)$$

$$\left.\begin{aligned} \varepsilon_i^{occ} &= \varepsilon_i^{LDA} - U/2 \\ \varepsilon_i^{emp.} &= \varepsilon^{LDA} + U/2 \end{aligned}\right\} \Delta\varepsilon = U$$

THEORY LEVELS